Physics and Imaging in Radiation Oncology 34 (2025) 100763

Contents lists available at ScienceDirect

Physics and Imaging in Radiation Oncology

journal homepage: www.sciencedirect.com/journal/physics-and-imaging-in-radiation-oncology

Original Research Article

Spot-optimization reduces beam delivery time in liver breath hold intensity modulated proton therapy

Michael Butkus [a,*], Daniel Bastawros [a], Yunze Yang [a], Roberto Cassetta [b], Roni Hytonen [c], Robert Kaderka [a]

[a] Department of Radiation Oncology, University of Miami Miller School of Medicine, Sylvester Comprehensive Cancer Center, Miami, FL, USA
[b] Varian, A Siemens Healthineers Company, Baden, Switzerland
[c] Varian, A Siemens Healthineers Company, Helsinki, Finland

ARTICLE INFO

Keywords:
Proton therapy
Treatment efficiency
Liver irradiation

ABSTRACT

Background and purpose: Liver irradiations with intensity-modulated proton therapy (IMPT) often require motion mitigation techniques that prolong treatment. A prototype spot-optimization algorithm was tested to evaluate whether plan delivery time could be reduced while preserving quality.

Methods and materials: Fifteen patients previously treated with liver IMPT using breath-hold were re-planned with nominal treatment planning system (TPS) settings and using a prototype spot-optimization algorithm in which combinations of minimum Monitor Unit (MU) and layer-spacing settings were tested: 1MU/1MeV, 3MU/3MeV, 1MU/5MeV, 5MU/3MeV. Spot-optimized and nominals plans were compared using standard dose-volume histogram (DVH) metrics for targets and organs-at-risk. A Wilcoxon signed-rank test was applied ($p < 0.05$). Delivery time for all plans were measured by creating and delivering IMPT quality assurance (QA) plans. Gamma analyses were performed on all plans to test deliverability. Plans were considered deliverable if >90 % of points passed a gamma criterion of 3 %/3mm.

Results: Minimal DVH differences were observed between nominal and spot-optimized plans. For the 3MU/3MeV setting, no DVH metrics were significantly different. Median and interquartile range (IQR) delivery times for these plans were 40 % (38 %–44 %) faster than nominal plans. 5MU/3MeV plans had median (IQR) delivery times 59 % (52 %–61 %) faster than nominal plans but had a small but significant increase in $Liver_{Eff}$ D_{mean} with a median (IQR) difference of 0.2 Gy(RBE) (0.0–0.4 Gy(RBE)). QA analysis showed all spot-optimized plans were deliverable.

Conclusions: The spot-optimization algorithm produced clinically deliverable plans with negligible DVH differences to nominal plans and reduced delivery time of liver IMPT by over one-third.

1. Introduction

Standard external beam radiation treatment of the liver is typically done with photon therapy. Proton therapy has the potential to substantially reduce dose outside of the target in liver cancer treatments and thus decrease side effects experienced by patients, notably radiation induced liver damage (RILD) [1–4]. The favorable dose distribution of protons depositing minimal dose after the Bragg peak and the small number of beam angles in proton therapy leaves large parts of the normal liver virtually without dose. However, due to respiration, the liver is susceptible to motion during treatments. When using intensity-modulated proton therapy (IMPT) this may result in unacceptable dose distributions due to the interplay effect [5–7]. Centers treating liver with IMPT therefore need to employ motion mitigation techniques to ensure adequate dose delivery [8]. Techniques for motion mitigation include abdominal compression [9,10], breath-holding (BH) [8,11], phase gating [12–14], re-painting [6,15], or a combination of these approaches. However, all the techniques mentioned decrease patient comfort and/or prolong treatment time.

Treatment using BH can reduce the interplay effect and thus result in better plan quality but can be difficult to tolerate for patients. Many patients have poor performance status and struggle maintaining reproducible breath holds. In IMPT, the amount of breath holds needed depends on target size and field arrangements and ranges from one to low

* Corresponding author at: 1475 Northwest 12th Avenue, Suite C123, Miami, FL 33136, USA.
E-mail address: butkus.michael@miami.edu (M. Butkus).

https://doi.org/10.1016/j.phro.2025.100763
Received 5 September 2024; Received in revised form 28 March 2025; Accepted 28 March 2025
Available online 3 April 2025

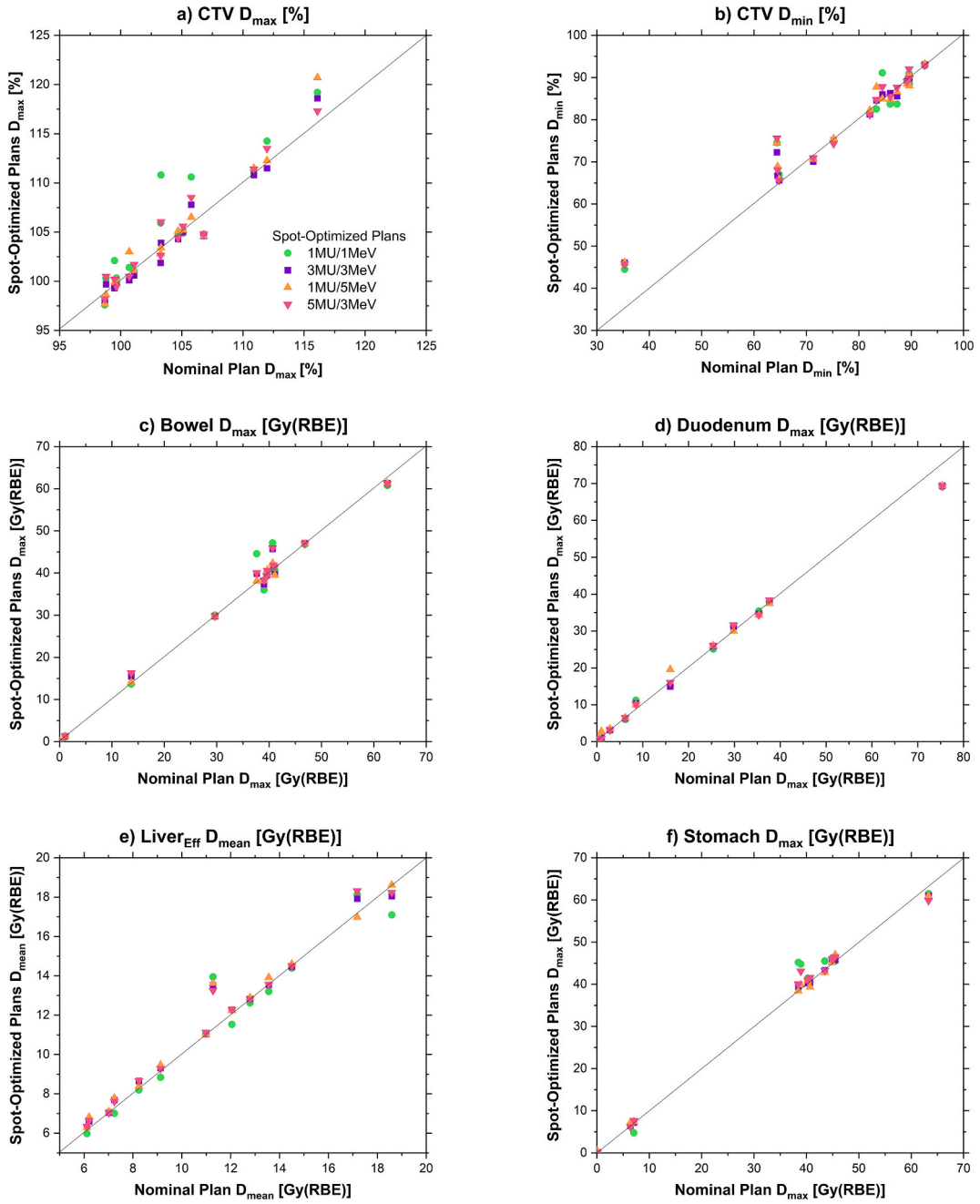

Fig. 1. Dose-volume parameters resulting from nominal plans and spot-optimized plans. Panels a-f (left-to-right, top-to-bottom), show parameters for CTV D_{max} (%), CTV D_{min} (%), Bowel D_{max} (Gy(RBE)), Duodenum D_{max} (Gy(RBE)), $Liver_{Eff}$ D_{mean} (Gy(RBE)), and Stomach D_{max} (Gy(RBE)).Values on the x-axis represent the nominal plans, y-values the spot-optimized plans. Points above the equivalence line thus indicate a higher dose when using the different spot-optimization settings.

double digits per field. An increased number of breath holds can lead to patient fatigue and anxiety, prolonging treatment time and reducing reproducibility, comfort, and ultimately, treatment quality.

Therefore, reducing the number of breath holds needed could substantially increase efficiency, quality and patient comfort. While there is ongoing research in increasing IMPT dose rate [16,17], machines in current clinical operation can often not increase dose rate without additional hardware upgrades. However, accounting for the machine specifications in plan optimization could be used to create plans that can be delivered faster on current machines [18–21].

Current iterations of IMPT optimization algorithms typically do not optimize delivery time. In this study, we evaluated a prototype beam optimization algorithm which uses spot-optimization. We investigated whether taking minimum Monitor Units (MU) and energy layer-spacing explicitly into account during the optimization process would reduce delivery time. We evaluated the performance of this prototype algorithm for liver IMPT in terms of plan quality, plan delivery time, and plan deliverability.

2. Materials and methods

2.1. Patients

Under a retrospective Institutional Review Board (IRB) approved protocol, we identified 15 consecutive liver patients that were previously treated at our institution with IMPT and BH. These patients included a variety of target sizes, fractionation schemes and planning techniques. For all plans a proton relative biological effectiveness (RBE)

Table 1
Dose-volume parameters from the nominal plans and different spot optimization settings. Nominal column shows median (IQR) plan values, other columns show the median (IQR) of the differences from the spot optimization plans and the nominal plan. Asterisk (*) denotes a statistically significant difference to nominal plans ($p < 0.05$).

Parameter	Nominal	*1MU/1MeV*	*3MU/3MeV*	*1MU/5MeV*	*5MU/3MeV*
Body D_{max} [%]	105 (103–111)	0 (0–2)*	0 (−1–0)	0 (−1–1)	0 (−1–2)
CTV D_{max} [%]	103 (100–106)	0 (0–3)*	−1 (0–0)	0 (0–0)	0 (0–0)
CTV V_{105} [%]	0 (0–0)	1 (0–3)*	0 (−1–0)	0 (0–1)	1 (0–1)
CTV D_{min} [%]	83 (66–88)	0 (−1–2)	1 (0–1)	0 (−1–3)	0 (0–3)
Bowel D_{max} [Gy(RBE)]	39.3 (17.7–40.8)	0.0 (−0.1–0.2)	0.2 (−0.1–0.8)	0.2 (0.0–0.8)	0.2 (0.0–1.0)
Duodenum D_{max} [Gy(RBE)]	12.3 (2.4–31.2)	−0.1 (−0.4–0.3)	0.1 (−0.2 to 0.4)	0.4 (0.0–0.9)	0.1 (−0.1–0.7)
Heart D_{mean} [Gy(RBE)]	1.1 (0.5–2.1)	−0.1 (−0.1–0.1)	0.0 (0.0–0.1)	0.0 (0.0–0.2)	0.0 (0.0–0.1)
Kidney R D_{mean} [Gy(RBE)]	0.1 (0.0–0.1)	0.0 (0.0–0.0)	0.0 (0.0–0.0)	0.0 (0.0–0.1)	0.0 (0.0–0.0)
$Liver_{Eff}$ D_{mean} [Gy(RBE)]	11.3 (7.7–14.0)	−0.1 (−0.3–0.1)	0.2 (0.0–0.4)	0.2 (0.1–0.5)*	0.2 (0.0–0.4)*
Spinal Cord D_{max} [Gy(RBE)]	1.0 (0.3–3.5)	−0.1 (−0.6–0.0)	0.1 (0.0–0.4)	0.1 (0.0–0.3)	0.2 (0.0–0.3)
Stomach D_{max} [Gy(RBE)]	38.9 (6.4–43.5)	0.0 (−0.1–1.3)	0.0 (−0.2–0.1)	0.3 (0.0–0.7)	0.6 (0.0–1.0)

of 1.1 was used and the per-fraction dosage varied from 3–7 Gy(RBE)[1] (median: 4 Gy(RBE)). Target volumes varied from 60–2302 cm^3 (median: 141 cm^3) and both single-field optimization and multi-field optimization plans were used. All relevant patient data was anonymized and exported to a system with the prototype algorithm. Our institution's dosimetric beam data and other clinical settings were copied into this external environment to emulate our treatment machine and to allow for delivery of the created plans on our treatment machine.

2.2. Spot-optimization

For each patient, several sets of plans were created. A *nominal* reference plan was generated using Eclipse non-uniform proton optimizer (NUPO) V.18 (Varian Medical Systems, Palo Alto, California, USA). The optimization of the nominal plans was identical to the way plans were generated in our clinic. When optimizing treatment plans, NUPO V.18 created a proton fluence with preset fixed energy layer-spacing. After the optimization, a post-processing step adjusted each spot in the plan to comply with machine limitations. The machine limitations set in our clinic were 3 MeV fixed layer-spacing and a minimum MU of 1, which corresponded to a Bragg peak dose-area product of 0.012–0.013 Gy(RBE) $\cdot cm^2$, depending on beam energy.

The prototype algorithm, called RapidScan (Varian Medical Systems, Palo Alto, California, USA) is an extension of NUPO V.18 that allows the user to enter a minimum MU and layer-spacing setting which will then be taken into account during spot-optimization (in contrast to this being a post-processing step without spot-optimization). By reducing the number of lowly-weighted (i.e. low MU) spots and energy layers in a plan the delivery time could possibly be reduced. The spot-optimization is implemented by adding a term to the optimization cost-function penalizing spots that violate the chosen settings. A strength setting is given to the user which determines the weight of this cost term. The strength is converted to weight using a non-linear function proportional to $Strength^n$ with $n = 5$.

For this study, we created a treatment plan with our clinical parameterization (1MU/3MeV) and four *spot-optimized* plans with the following minimum MU and layer-spacing settings: 1MU/1MeV, 3MU/3MeV, 1MU/5MeV, and 5MU/3MeV. These settings explored the effects of both changing the minimum MU and layer-spacing. Ideally, an optimal choice of parameters would result in high quality plans and fast delivery time. The 1MU/1MeV scenario was added to test whether the additional degrees of freedom in layer-spacing during optimization would improve plan quality compared to nominal plans. A fixed strength of 75 was used for the spot-optimization objectives; the effect of changing the strength was not investigated. Aside from the parameters specific to spot-optimization, all objectives and robustness settings in the optimization were identical to the nominal plans. We employed robust optimization on target parameters with ±3.5 % range uncertainty and ±5 mm setup uncertainties in all directions. After optimization, the nominal plans were normalized to the same $V_{95\%}$ that was used clinically.

2.3. Plan delivery time and plan deliverability

Our patient-specific IMPT quality assurance (QA) workflow was used to evaluate delivery time and test plan deliverability. Plans were exported from the prototype environment into our clinical environment for delivery on our proton machine, a Varian ProBeam Compact system. QA plans were generated which keep spot, MU, and range shifter settings identical to the patient plans but override gantry angles to zero. These plans were irradiated onto a IBA Matrixx detector (IBA Dosimetry GmbH, Schwarzenbruck, Germany) underneath a stack of solid water (stack size dependent on approximate target depth).

Plan delivery time was measured with a stopwatch. Plan deliverability was assessed by comparing field-by-field planned and measured dose using a gamma index [22] of 3 %/3mm with a goal of >90 % passing. This represents our clinical IMPT QA passing criterion.

2.4. Plan comparison and statistical analysis

The nominal plans were considered the reference plans, as those represent current clinical practice. Statistical significance of the differences of several dose-volume metrics were assessed with a Wilcoxon signed-rank test ($p < 0.05$) between the nominal and spot-optimized plans. Dose-volume metrics were CTV $V_{105\%}$, CTV D_{max}, CTV D_{min}, non-involved effective Liver ($Liver_{Eff}$) D_{mean}, Bowel D_{max}, Duodenum

[1] Gy(RBE) refers to nomenclature of International Commission on Radiation Units and Measurements (ICRU) Report 93: Prescribing, Recording, and Reporting Light Ion Beam Therapy (https://doi.org/10.1093/jicru_ndy025).

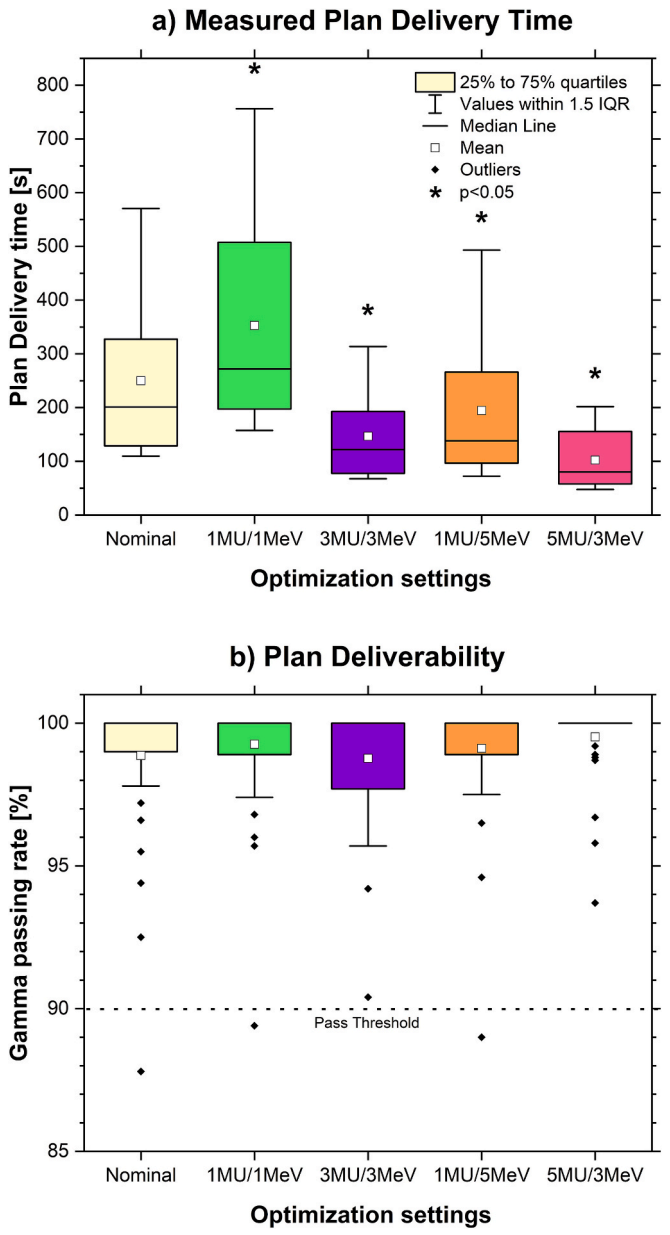

Fig. 2. Boxes illustrate the quartile ranges for 25 % to 75 % of the values, whiskers show values within 1.5x the interquartile range, line depicts median value, square the mean value, black diamonds represent outliers, asterisks denote significant difference to nominal plans ($p < 0.05$). TOP: Plan delivery times measured for nominal and spot-optimized plans. c) Gamma passing rates for the nominal and spot-optimized plans with 3 %/3mm fields.

D_{max}, Heart D_{mean}, Kidney R D_{mean}, Stomach D_{max}, and Spinal cord D_{max}. Reported dose differences are the median and interquartile range (IQR) differences between the nominal and spot-optimized plans.

Plan delivery and spot-analysis metrics were analyzed similarly to dose-volume metrics. Plan delivery metrics were delivery time and gamma passing rates. The spot analysis was completed using an in-house script (Matlab 2023a, MathWorks, MA, USA) that reports total number of spots and energy layers, as well as the minimum, arithmetic mean, and maximum MU of all plans. Median and IQR are reported for these metrics.

Robustness was assessed as a binary "acceptable or not" based on clinical judgement. Analytical comparative tests between robustness of nominal and spot-optimized plans were not completed.

3. Results

3.1. Plan comparison

Overall, differences in dose-volume metrics between the optimization techniques were minimal (Fig. 1). Compared to nominal plans, the only significant differences were an increase in Body and CTV D_{max} with median (IQR) differences of 1 % (0 %–2%) and 1 % (0 %–3%), respectively, when using the 1MU/1MeV setting, and an increase in $Liver_{Eff}$ D_{mean} for 1MU/5MeV and 5MU/3MeV spot-optimized plans. The median (IQR) differences for these were 0.2 Gy(RBE) (0.1–0.5 Gy(RBE)) and 0.2 Gy(RBE) (0.0–0.4 Gy(RBE)), respectively. Differences of organs-at-risk on average were below 1 Gy(RBE) compared to the nominal plans. With respect to the CTV, the spot-optimization showed an increase in both max and min dose, but differences again were not significant ($p > 0.05$ for all comparisons) (Table 1).

The increased degrees of freedom by giving the optimizer a 1 MeV layer-spacing with the 1MU/1MeV setting did not result in increased plan quality. In fact, there were several plans where the 1MU/1MeV setting resulted in higher OAR dose ($p > 0.05$ for all comparisons). Evaluations of plan robustness resulted in no clinically relevant differences between the different optimization techniques and the robustness of all plans was deemed acceptable.

3.2. Plan delivery time and plan deliverability

The median (IQR) delivery time for nominal plans was 201 s (130–313 s). Optimizing with 1MU/1MeV resulted in median (IQR) delivery times 40 % (32 %–59 %) longer than the nominal plans. Optimization with 3MU/3MeV, 1MU/5MeV, and 5MU/3MeV resulted in median (IQR) delivery times 40 % (38 %–44 %), 26 % (13 %–33 %), and 59 % (52 %–61 %) faster than nominal plans, respectively. All differences to nominal plans were statistically significant (Fig. 2).

From these results, it appears that changing the minimum spot-weight setting to 3 MU in spot-optimization has the largest relative effect on delivery time compared to nominal plans. The switch from a minimum of 3 MU to 5 MU resulted in additional gains in delivery speed. Using a 5 MeV layer-spacing instead of the standard 3 MeV had a smaller impact on delivery time than adjusting the MU settings (Table 2).

Differences in gamma pass rates for delivered plans were not significant for the 3 %/3mm criterion ($p > 0.05$). All fields of the spot-optimized plans with 3MU/3MeV and 5MU/3MeV setting passed the $\gamma > 90$ % for 3 %/3mm criterion used in our patient-specific IMPT QA workflow and were thus considered deliverable. For the nominal plans, as well as 1MU/1MeV and 1MU/5MeV plans one field across the cohort each failed our QA with rates of 88–89 % (Fig. 2).

3.3. Spot analysis

For the nominal plans, the median (IQR) mean spot weight was 7 MU (6–10 MU). Spot-optimization significantly decreased the median (IQR) mean spot weight for 1MU/1MeV plans to 4 MU (3–5 MU) and significantly increased it for 3MU/3MeV, 1MU/5MeV and 5MU/3MeV plans to 9 MU (7 –11 MU), 9 MU (7–14 MU), and 11 MU (9–13 MU), respectively (Fig. 3).

Maximum spot weights were also significantly increased from 163 MU (107–223 MU) in nominal plans to 291 MU (150–354 MU) in 3MU/3MeV plans, 298 MU (190–324 MU) in 1MU/5MeV plans, and 242 MU (162–376 MU) in 5MU/3MeV plans. In two cases for the 3MU/3MeV plans, and in one case each for the 1MU/5MeV and 5MU/3MeV plans, the maximum MU exceeded 500 MU in a single spot.

The median (IQR) number of spots decreased from 2832 (1755–3689) in nominal plans to 2748 (1434–3431) in 3MU/3MeV plans, though this difference was not significant. In contrast, the increase observed in 1MU/1MeV plans to 5698 (3107–10092) spots, and the decrease observed in 1MU/5MeV 2093 (1350–4152) and 5MU/

Table 2
Delivery times and relevant plan parameters across different optimization settings. The table lists the number of fields, dose per fraction (fx), CTV volume, and the delivery time for the entire plan. Delivery times are shown for the nominal plan as well as the spot-optimized plans with the listed settings. Additionally, the final two rows show median and IQR for the differences in plan delivery time for spot-optimized plans compared to nominal plans. Values in parentheses indicate a decrease in delivery time relative to the nominal plans. Asterisk (*) denotes statistical significance ($p < 0.05$).

Patient #	Fields	Dose per fx [Gy(RBE)]	CTV Volume (cm^3)	Nominal [s]	1MU/1MeV [s]	3MU/3MeV [s]	1MU/5MeV [s]	5MU/3MeV [s]
1	3	5.0	83	110	193	77	89	53
2	2	4.0	113	113	158	68	72	47
3	3	3.3	62	125	208	90	76	77
4	2	4.0	141	129	187	78	97	53
5	2	4.0	60	131	198	77	124	58
6	3	3.0	152	150	252	113	97	80
7	4	7.0	97	187	272	116	138	76
8	3	4.5	411	201	280	124	132	71
9	3	4.0	95	214	269	122	198	87
10	2	6.0	138	238	305	131	209	92
11	4	4.0	473	298	508	183	266	149
12	3	3.0	752	327	431	193	222	156
13	3	4.5	855	428	576	235	312	165
14	3	4.0	2302	532	700	280	393	172
15	3	4.0	2299	571	756	314	493	202
Median	3	4.0	141	201	272	122	138	92
IQR	2–3	4.0–4.5	96–613	130–313	203–470	84–188	97–244	65–153
Difference between Spot-Optimized and Nominal Plan Delivery Time					**1MU/1MeV**	**3MU/3MeV**	**1MU/5MeV**	**5MU/3MeV**
Median					+40 %*	(40 %)*	(26 %)*	(59 %)*
IQR					32 %–59 %	(38 %–44 %)	(32 %–59 %)	(32 %–59 %)

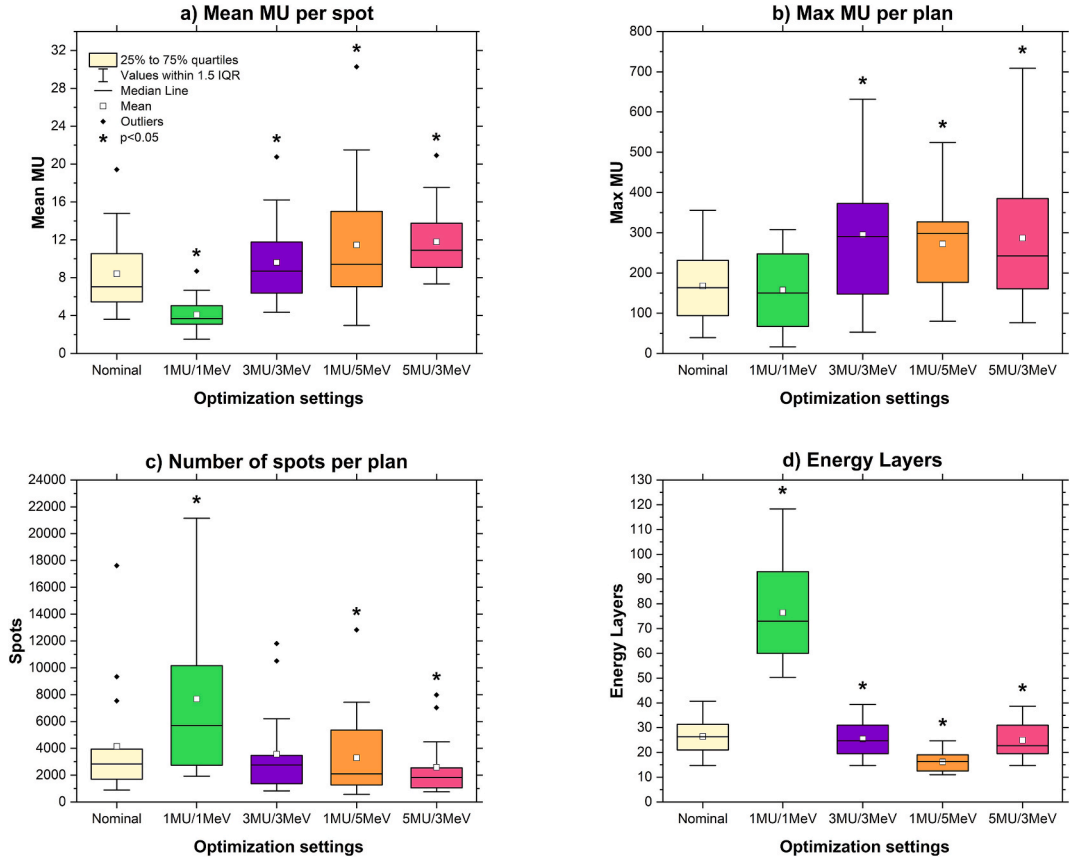

Fig. 3. Boxplots analyzing the a) Mean MU per spot, b) Max MU per plan, c) number of spots per plan, and d) number of energy layers per plan for the nominal and spot-optimized plans. Asterisk denotes significant difference to nominal plans ($p < 0.05$).

3MeV 1808 (1148–2488) spots, were significant. All changes in number of energy layers per plan were significant: nominal plans used 26 (21–31) layers, while 1MU/1MeV used 73 (61–90), 3MU/3MeV used 25 (20–30), 1MU/5MeV used 16 (13–19), and 5MU/3MeV used 23 (20–30).

Minimum MUs for all plans matched the minimum MU settings in the optimization (1 MU for the nominal, 1MU/1MeV, and 1MU/5MeV plans, 3MU for 3MU/3MeV plans and 5MU for 5MU/3MeV).

4. Discussion

In this study, median (IQR) delivery time of IMPT liver BH treatments was shown to decrease by 40 % (38 %–44 %) when using spot-optimization with 3 MU minimum and 3 MeV layer-spacing settings, compared to nominal settings. No significant changes in plan quality were seen for this parameterization. The 5MU/3MeV setting showed additional time savings but a slight increase in $Liver_{Eff}$ D_{mean} dose. This highlights the need for clinical assessment to evaluate whether the additional time savings is an acceptable trade-off for the increased dose to the liver.

The spot analysis indicated that the 3MU/3MeV spot-optimization significantly increased mean and maximum spot weights, while the total number of spots decreased but not significantly. All parameters were significantly increased for the 1MU/5MeV and 5MU/3MeV plans. Proton therapy planners generally attempt to avoid excessive weight in single spots to reduce the risk of local toxicity, heterogeneous dose distributions, and uncertainty during delivery. Therefore, it is advisable for planners using this new, or similar, algorithm(s) to monitor plans for highly weighted spots and assess clinical concern on a per-treatment basis. Future iterations of the spot-optimization algorithm should implement a feature for planners to set a maximum MU during optimization.

Our results are in general agreement with previous studies [19–21,23,24] that have investigated the temporal implications from adjustments in IMPT delivery dynamics. Although these investigations vary by treatment sites, tumor sizes, and delivery machines, the common theme of a possible reduction in delivery time (ranging from approximately 20–50 %) with no, or minimal, loss of plan quality is similar. Collectively, these results suggest that the high degeneracy [25] of current optimization algorithms are able to overcome certain constraints on the degrees-of-freedom in IMPT planning.

Zhu [21] et al. investigated the effect of energy layer variation in the reduction of treatment time for 7 patients and delivered those plans on a machine similar to this study. Their median (IQR) reduction of nominal to fastest reported treatment times, normalized to target volume size and dose level, was 32 % (25 %–33 %) while ours was 59 % (52 %–61 %). The greater reduction on similar, cyclotron-based, treatment machines may illustrate that the increase in minimum MU could potentially play a larger role in decreasing delivery times than energy-layer spacing for cyclotron systems as the nozzle current is generally controlled by the minimum MU per energy layer [20]. Essentially, increasing the minimum MU allows for the system to operate at a higher effective dose-rate, ergo decreasing delivery time. For slower energy-layer switching deliveries, such as synchrotrons, greater energy-layer spacing may have a greater impact on delivery time.

This study had several limitations. The planning study was performed with identical optimization parameters across all spot-optimization settings, namely a 75-strength objective on the minimum MU setting. The intent of using a constant strength setting for all plans was to investigate how much time saving could be expected with minimal changes to a typical planning workflow. However, it is possible that varying strength setting may result in a more optimal setting which yields faster delivery and/or higher plan quality. As a further limitation, the current version of the algorithm does not allow for adaptive energy-layer settings per energy-layers as suggested in previous studies [21].

The scope of this study focused on the plan delivery time itself. This represents only a fraction of the time patients spend on the couch. Time for setup, imaging, and gantry movement was not considered. However, plan delivery is typically the most strenuous aspect of the treatment, especially when requiring breath holds. Breath hold duration is highly patient-specific, but assuming a 30 s breath hold the longest treatment in our cohort would have required 19 breath holds for 571 s of treatment with nominal plans. Using the 3MU/3MeV plan this would be reduced to just 11 breath holds for a treatment time of 314 s. The prototype status of this algorithm means that translating these findings into the clinic requires careful commissioning by medical physicists and planners to ensure expected results when using the final iteration of the algorithms. As a further limitation, this study and its findings are limited to liver treatments. It is possible that other disease sites may need different optimization settings to achieve high plan quality and should thus be evaluated further. This may be especially true for the evaluation of robustly optimized plans. Robust optimizations were undertaken for all plans and reviewed as a simple “acceptable or not” basis, very minor differences in robustness metrics were seen.

On the other hand, this focus on liver also represents one of the strengths of this study. Previously published studies investigated a single or a few plans for multiple disease sites [19–21]. In this study a comprehensive review across a diverse liver patient cohort and multiple optimization settings was performed. While careful review is always prudent when using new technology, the results presented give clinics a practical guide on how to quickly implement spot-optimization into routine clinical care with minimal changes to the current workflow.

Previous studies discussed delivery time optimization algorithms modulating energy-layers [18,21], minimum MU settings [20] or both [19] but lacked time, and or, dose measurements of actually delivered fields. The present study expands on these findings and adds dose measurements of actual plan delivery, similar to a full end-to-end test of a new algorithm [26].

In summary, we demonstrated that the prototype spot-optimization algorithm could reduce delivery time for liver IMPT patients by approximately one third using a 3MU/3MeV setting with minimal consequences. Additional time savings were possible with the 5MU/3MeV setting albeit with a slight increase in dose to the unaffected liver. These reductions could substantially increase patient comfort and treatment efficiency, particularly for breath-hold patients, reducing the burden on the patient, staff, and machine. Future research should explore varying strength settings and application to other disease sites to further validate these findings.

Declaration of competing interest

The authors declare that they have no known competing financial interests or personal relationships that could have appeared to influence the work reported in this paper.

References

[1] Mondlane G, Gubanski M, Lind PA, Ureba A, Siegbahn A. Comparative study of the calculated risk of radiation-induced cancer after photon- and proton-beam based radiosurgery of liver metastases. *Phys Med* 2017;42:263–70. https://doi.org/10.1016/j.ejmp.2017.03.019.

[2] Mondlane G, Ureba A, Gubanski M, Lind PA, Siegbahn A. Estimation of the risk for radiation-induced liver disease following photon- or proton-beam radiosurgery of liver metastases. *Radiat Oncol* 2018;13:206. https://doi.org/10.1186/s13014-018-1151-6.

[3] Dionisi F, Ben-Josef E. The use of proton therapy in the treatment of gastrointestinal cancers: Liver. *Cancer J* 2014;20:371–7. https://doi.org/10.1097/PPO.0000000000000082.

[4] Siddiqui O, Pollock A, Samanta S, Kaiser A, Molitoris JK. Proton beam therapy in liver malignancies. *Curr Oncol Rep* 2020;22:30. https://doi.org/10.1007/s11912-020-0889-9.

[5] Fracchiolla F, Dionisi F, Righetto R, et al. Clinical implementation of pencil beam scanning proton therapy for liver cancer with forced deep expiration breath hold. *Radiother Oncol* 2021;154:137–44. https://doi.org/10.1016/j.radonc.2020.09.035.

[6] Zhang Y, Huth I, Wegner M, Weber DC, Lomax AJ. An evaluation of rescanning technique for liver tumour treatments using a commercial PBS proton therapy system. *Radiother Oncol* 2016;121:281–7. https://doi.org/10.1016/j.radonc.2016.09.011.

[7] Lebbink F, Stocchiero S, Fossati P, et al. Parameter based 4D dose calculations for proton therapy. *Phys Imaging Radiat Oncol* 2023;27:100473. https://doi.org/10.1016/j.phro.2023.100473.

[8] Zhang Y, Trnkova P, Toshito T, et al. A survey of practice patterns for real-time intrafractional motion-management in particle therapy. *Phys Imaging Radiat Oncol* 2023;26:100439. https://doi.org/10.1016/j.phro.2023.100439.

[9] Eccles CL, Dawson LA, Moseley JL, Brock KK. Interfraction liver shape variability and impact on GTV position during liver stereotactic radiotherapy using abdominal compression. *Int J Radiat Oncol Biol Phys* 2011;80:938–46. https://doi.org/10.1016/j.ijrobp.2010.08.003.

[10] Hu Y, Zhou YK, Chen YX, Zeng ZC. Magnitude and influencing factors of respiration-induced liver motion during abdominal compression in patients with intrahepatic tumors. *Radiat Oncol* 2017;12:9. https://doi.org/10.1186/s13014-016-0762-z.
[11] Guo B, Stephans K, Woody N, Antolak A, Moazzezi M, Xia P. Online verification of breath-hold reproducibility using kV-triggered imaging for liver stereotactic body radiation therapy. *J Appl Clin Med Phys* 2023;24:e14045. https://doi.org/10.1002/acm2.14045.
[12] Giraud P, Houle A. Respiratory gating for radiotherapy: main technical aspects and clinical benefits. *ISRN Pulmonol* 2013;2013:519602. https://doi.org/10.1155/2013/519602.
[13] Wagman R, Yorke E, Ford E, et al. Respiratory gating for liver tumors: use in dose escalation. *Int J Radiat Oncol Biol Phys* 2003;55:659–68. https://doi.org/10.1016/s0360-3016(02)03941-x.
[14] Oh SA, Yea JW, Kim SK, Park JW. Optimal gating window for respiratory-gated radiotherapy with real-time position management and respiration guiding system for liver cancer treatment. *Sci Rep* 2019;9:4384. https://doi.org/10.1038/s41598-019-40858-2.
[15] Poulsen PR, Eley J, Langner U, Simone CB, Langen K. Efficient interplay effect mitigation for proton pencil beam scanning by spot-adapted layered repainting evenly spread out over the full breathing cycle. *Int J Radiat Oncol Biol Phys* 2018;100:226–34. https://doi.org/10.1016/j.ijrobp.2017.09.043.
[16] Hughes JR, Parsons JL. FLASH radiotherapy: current knowledge and future insights using proton-beam therapy. *Int J Mol Sci* 2020;21:6492. 10.3390ijms21186492.
[17] Zou W, Diffenderfer ES, Cengel KA, et al. Current delivery limitations of proton PBS for FLASH. *Radiother Oncol* 2021;155:212–8. https://doi.org/10.1016/j.radonc.2020.11.002.
[18] Jensen MF, Hoffmann L, Petersen JBB, Møller DS, Alber M. Energy layer optimization strategies for intensity-modulated proton therapy of lung cancer patients. *Med Phys* 2018;45:4355–63. https://doi.org/10.1002/mp.13139.
[19] Lin Y, Clasie B, Liu T, McDonald M, Langen KM, Gao H. Minimum-MU and sparse-energy-layer (MMSEL) constrained inverse optimization method for efficiently deliverable PBS plans. *Phys Med Biol* 2019;64:205011. https://doi.org/10.1088/1361-6560/ab4529.
[20] Gao H, Clasie B, McDonald M, Langen KM, Liu T, Lin Y. Technical Note: Plan-delivery-time constrained inverse optimization method with minimum-MU-per-energy-layer (MMPEL) for efficient pencil beam scanning proton therapy. *Med Phys* 2020;47:3892–7. https://doi.org/10.1002/mp.14363.
[21] Zhu M, Flampouri S, Stanforth A, et al. Effect of initial energy layer and spot placement parameters on IMPT delivery efficiency and plan quality. *J Appl Clin Med Phys* 2023;24:e13997. https://doi.org/10.1002/acm213997.
[22] Low D, Harms W, Mutic S, Purdy J. A technique for the quantitative evaluation of dose distributions. *Med Phys* 1998;25:656–61. https://doi.org/10.1118/1.598248.
[23] van de Water S, Belosi M, Albertini F, Winterhalter C, Weber D, Lomax A. Shortening delivery times for intensity-modulated proton therapy by reducing the number of proton spots: an experimental verification. *Phys Med Biol* 2020;65:095008. https://doi.org/10.1088/1361-6560/ab7e7c.
[24] Yi B, Mossahebi S, Jatczak J, et al. Optimial minimum MU for intensity-modulated proton therapy with pencil-beam scanning proton beams. *J Appl Clin Med Phys* 2024;25:e14435. https://doi.org/10.1002/acm2.14435.
[25] Alber M, Meedt G, Nusslin F, Reemtsen R. On the degeneracy of IMRT optimization problem. *Med Phys* 2002;29:2584–9. https://doi.org/10.1118/1.1500402.
[26] Geurts M, Jacqmin D, Jones L, et al. AAPM medical physics practice guideline 5.b: commissioning and QA of treatment planning dose calculations-meagvoltage photon and electron beams. *Med Phys* 2022;23:e13641. https://doi.org/10.1002/acm2.13641.